Available online at www.sciencedirect.com
ScienceDirect
Journal of Molecular Catalysis A: Chemical 266 (2007) 166–172
JOURNAL OF MOLECULAR CATALYSIS A: CHEMICAL
www.elsevier.com/locate/molcata

Poisoning effect of sulphate on the selective catalytic reduction of NO_x by C_3H_6 over Ag-Pd/Al_2O_3

Shuxia Xie, Jin Wang, Hong He *

State Key Laboratory of Environmental Chemistry and Ecotoxicology, Research Center for Eco-Environmental Sciences, Chinese Academy of Sciences, Beijing 100085, China

Received 2 May 2006; received in revised form 11 October 2006; accepted 26 October 2006
Available online 4 December 2006

Abstract

The Ag-Pd/Al_2O_3 catalyst showed a higher NO_x conversion than Ag/Al_2O_3 in the selective catalytic reduction (SCR) of NO_x by C_3H_6 especially at temperatures ranging from 573 to 773 K. However, the presence of SO_2 in the feed gas decreased the activity of NO_x reduction over Ag-Pd/Al_2O_3 more greatly than that over Ag/Al_2O_3. The sulphate species formed on the poisoned Ag-Pd/Al_2O_3 and Ag/Al_2O_3 were characterized by BET, inductively couple plasma optical emission spectrometer (ICP-OES), XRD, temperature programmed desorption (TPD) and in situ diffuse reflectance infra-red fourier transform spectroscopy (DRIFTS) methods. Two kinds of sulphate species were found on the SO_2 poisoned Ag-Pd/Al_2O_3 catalyst, and the formation of nitrate was blocked by the surface sulphate species. The addition of Pd into Ag/Al_2O_3 promoted the formation of sulphate on the Ag sites in the presence of SO_2, which was considered to be the possible reason for the weak sulphur resistance of Ag-Pd/Al_2O_3.

Keywords: Ag-Pd/Al_2O_3; Enolic species; In situ DRIFTS; Sulphate; TPD

1. Introduction

The selective catalytic reduction (SCR) of NO_x by hydrocarbons (HC-SCR) offers an attractive alternative to NH_3-SCR technology. The system of Ag/Al_2O_3-hydrocarbons for the SCR of NO_x has been reported by many researchers [1–7] for its high selectivity. However, the activity of Ag/Al_2O_3 at low temperatures needs to be improved for practical usage. Our recent work [8] showed that the addition of 0.01 wt% Pd into the 5wt% Ag catalyst (denoted as Ag-Pd/Al_2O_3) increases its catalytic activity for the SCR of NO_x at low temperatures; however, our work also showed the weak sulphur tolerance of the Ag-Pd/Al_2O_3 catalyst in the presence of SO_2 [9]. It should be noted that the presence of SO_2 in the various exhausts is another serious problem in catalytic after-treatment [10]. The tolerance of metal oxide-based catalysts to SO_2 depends on the type and oxidation state of the deposited metal, the nature of the support and the kind of reductants. Sumiya et al. [11] reported the suppression effect of SO_2 on the activity of Ag/alumina mounted on a cordierite was attributed to the formation of sulphate on the catalyst. Angelidis and Kruse [12] examined the promotion of the SCR of NO_x process by SO_2 over Ag/Al_2O_3 using C_3H_6/C_3H_8 as the reductant. Gandhi and Shelef [13] investigated the effect of sulphur compounds on the reduction of NO. They found that the dispersion of metal particles on the support was an important factor in the oxidation of SO_2, and that the activity of NO reduction to nitrogen and ammonia over the Pt and Pd catalysts was completely suppressed by the presence of very low levels of SO_2. They also concluded that under oxidizing conditions, the sulphur storage capability of the support in the form of sulphate directly affected the catalyst resistance to poisoning. However, the sulphate species characterization was insufficient and conclusive information of the effect of SO_2 on the catalysts is not in consensus due to the difference of reported results.

For obtaining more information about the sulphur resistance of SCR catalysts, the present study has been conducted to reveal the SO_2 deactivating mechanism of Ag-Pd/Al_2O_3 during C_3H_6-SCR of NO_x. We examined the time dependence of the activity of the SCR of NO_x on SO_2 when SO_2 was added into the feed gas, and the temperature programmed desorption (TPD) method was

* Corresponding author. Tel.: +86 10 62849123; fax: +86 10 62923563.
E-mail address: honghe@rcees.ac.cn (H. He).

1381-1169/$ – see front matter © 2006 Elsevier B.V. All rights reserved.
doi:10.1016/j.molcata.2006.10.055

used to identify the surface sulphate species. The in situ diffuse reflectance infra-red fourier transform spectroscopy (DRIFTS) method was used to detect the effect of SO_2 on the formation of key intermediates such as –NCO, enolic species, and NO_3^- under different reaction conditions.

2. Experimental

2.1. Catalyst preparation

The Ag/Al_2O_3 (Ag 5 wt%) and $Ag\text{-}Pd/Al_2O_3$ (Ag 5 wt%, Pd 0.01 wt%) catalysts were prepared by the impregnation method described in our earlier paper [8]. The poisoned Ag/Al_2O_3 and $Ag\text{-}Pd/Al_2O_3$ were prepared in the flow of 80 ppm SO_2 at 723 K for 10 h.

2.2. Catalyst characterization

Transmission electron microscopy (TEM) (JEOL/JEM-1200EX, 80 kV) was employed to examine the structure of the fresh and poisoned $Ag\text{-}Pd/Al_2O_3$ and Ag/Al_2O_3 powders. XRD profiles were measured using a D/MAX-RB diffractometer equipped with copper target X-ray tube($\lambda = 0.154$ nm). The X-ray source was operated at 2000 W (40 kV, 50 mA). The scans were performed over the range of 20–90° and at a scan rate of 3°/min. The surface area, pore volume and pore size of different catalysts were measured by using a Micromeritics TriStar 3000 apparatus. The surface area was determined by multi-point measurements using N_2 adsorption isotherms at 77 K. Elemental S analysis was operated by inductively couple plasma optical emission spectrometer (ICP-OES) method using a Perkin-Elmer OPTIMA 2000.

2.3. Catalytic tests

The catalytic test was carried out in a fixed-bed quartz flow reactor (10 mm i.d.) by passing a mixture of 800 ppm NO, 1714 ppm C_3H_6, 0–80 ppm SO_2 and 10 vol% O_2 in high pure N_2 at a rate of 4000 $cm^3\,min^{-1}$ over a 1.2 g catalyst ($W/F = 0.018\ g\,s\,cm^{-3}$; SV, ~50,000 h^{-1}). Ten volume percent H_2O vapor was supplied with a syringe pump and vaporized by a coiled heater set at the inlet of the reactor. Water was removed from the reactor effluent gas by passing it through a condenser before it reached the online analyzers. After reaching a steady state, the effluent gas was analyzed by a chemiluminescence $NO/NO_2/NO_x$ analyzer (42C-HL, Thermo Environmental) for NO_x conversion analysis. The activity was defined as NO_x conversion: NO_x conversion $= (NO_{x\,inlet} - NO_{x\,outlet})/NO_{x\,inlet}$.

2.4. TPD

All TPD measurements were performed using a quartz reactor coupled to a quadrupole mass spectrometer (Hiden HPR20) with a linear heating rate of 30 K min^{-1} in a He flow of 50 ml min^{-1}. Before the experiment, a 0.5 g fresh sample was ground into powder and pretreated in situ in 10% O_2 at 823 K for 2 h prior to experiments. For the SO_2-TPD, the catalyst was pretreated in the presence of 80 ppm SO_2 and 10% O_2 at 723 K for 10 h, and subsequently the catalyst was cooled to 303 K in the flow of N_2. For the NO-TPD, the fresh and pre-poisoned catalysts were treated in the flow of 800 ppm NO and 10% O_2 at 473 K for 1 h. The catalyst was then flushed with He for 30 min to remove physically adsorbed gas before commencement of temperature ramp.

2.5. In situ diffuse reflectance infra-red fourier transform spectroscopy procedure

In situ DRIFTS spectra were recorded on a NEXUS 670-FTIR instrument equipped with a smart collector and an MCT/A detector cooled by liquid N_2. The sample (ca. 30 mg) was finely ground and placed in a ceramic crucible. Prior to each experiment, the catalyst was thermally treated in a flow of 10 vol% $O_2 + N_2$ for 60 min at 573 and for another 60 min at 873 K, then cooled to the desired temperature, and a spectrum of the catalyst in the flow of $N_2 + O_2$ serving as the background was recorded. All spectra were measured under the simulated reaction conditions with a resolution of 4 cm^{-1} and an accumulation of 100 scans.

3. Results and discussion

3.1. Catalyst characterization

Fig. 1(a–d) shows the TEM images of fresh and poisoned $Ag\text{-}Pd/Al_2O_3$ and Ag/Al_2O_3 catalysts. Fig. 1(a and c) indicate that the typical sizes of metal Ag particles on fresh $Ag\text{-}Pd/Al_2O_3$ and Ag/Al_2O_3 are in the range of 5–15 nm, whereas the metal Ag sizes on SO_2 poisoned catalysts are obviously larger than that on the fresh catalyst. The metal Ag is assigned as an Ag single crystal by the electron diffraction pattern (in upper right of Fig. 1(b)). No Pd particle is observed on fresh and poisoned

Table 1
Surface area, pore volume, pore diameter and S content of γ-Al_2O_3, fresh and poisoned $Ag\text{-}Pd/Al_2O_3$ and Ag/Al_2O_3 catalysts

Sample	Surface area (m^2/g)	Pore volume (cm^3/g)	Pore diameter (nm)	S content (wt%)
γ-Al_2O_3	262	0.71	13.1	–
$Ag\text{-}Pd/Al_2O_3$	267	0.84	12.7	–
Poisoned $Ag\text{-}Pd/Al_2O_3$	219	0.68	12.5	1.37
Ag/Al_2O_3	245	0.71	11.5	–
Poisoned Ag/Al_2O	216	0.71	13.1	1.22

Poisoned $Ag\text{-}Pd/Al_2O_3$ and Ag/Al_2O_3 were prepared by treating fresh catalysts in the presence of 80 ppm SO_2 at 723 K for 10 h.

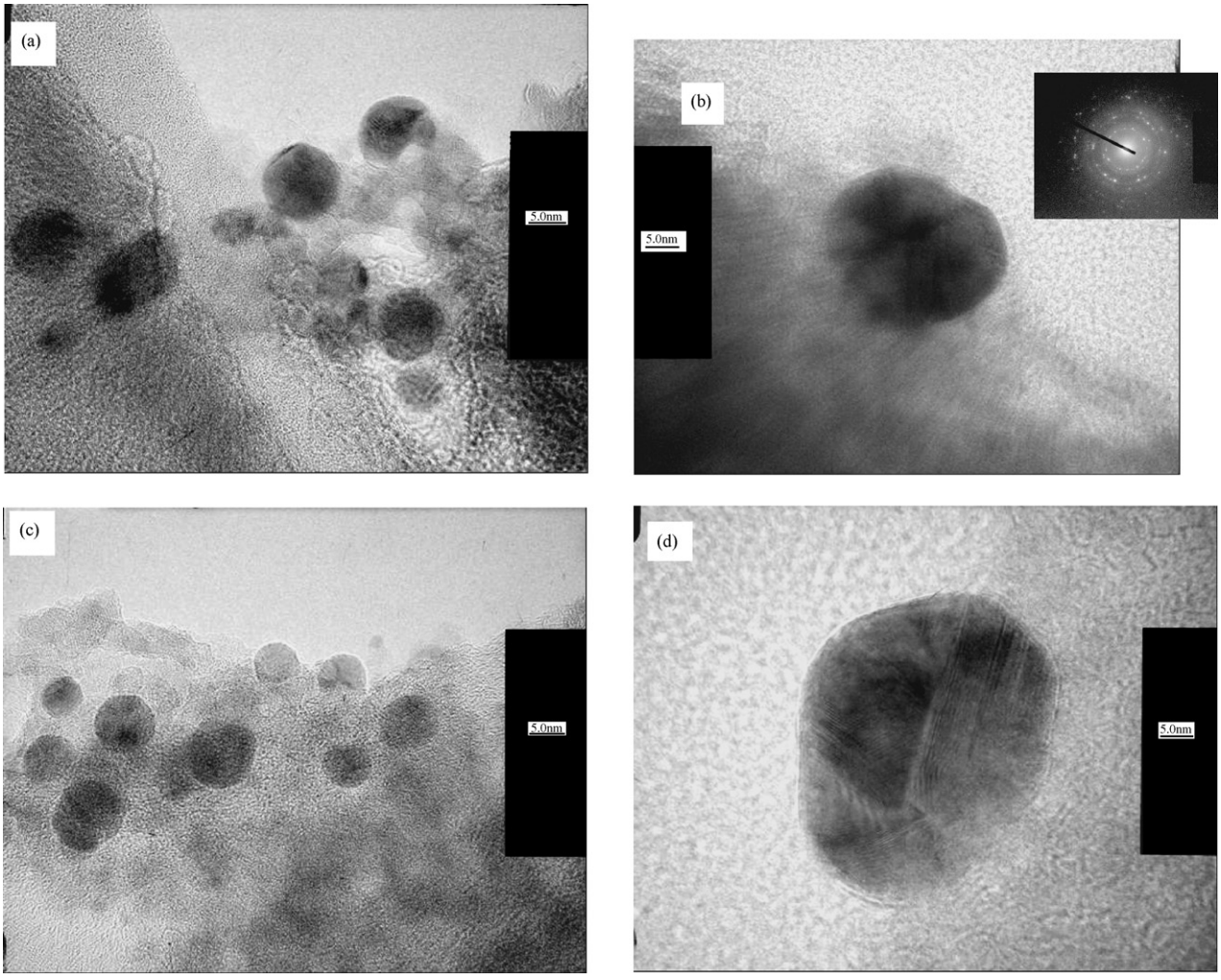

Fig. 1. TEM images of Ag-Pd/Al_2O_3 and Ag/Al_2O_3 particles: (a) fresh Ag-Pd/Al_2O_3, (b) SO_2 poisoned Ag-Pd/Al_2O_3, (c) fresh Ag/Al_2O_3 and (d) SO_2 poisoned Ag/Al_2O_3.

Ag-Pd/Al_2O_3, which is due to the fact that the addition amount of Pd is too small and that Pd is highly dispersed (<1 nm) on the catalyst surface.

Fig. 2 shows the XRD patterns of the fresh and poisoned catalysts of Ag-Pd/Al_2O_3 and Ag/Al_2O_3. The diffraction patterns of fresh Ag-Pd/Al_2O_3 and Ag/Al_2O_3 show only character of the support γ-Al_2O_3. Neither silver nor palladium oxide is detected, which indicates that the silver and palladium oxide particles are well dispersed over the catalyst. After Ag-Pd/Al_2O_3 is poisoned by 80 ppm SO_2 at 723 K for 10 h, sharp silver sulphate (Ag_2SO_4) peaks are observed. However, when Ag/Al_2O_3 catalyst is poisoned by SO_2 under the same condition as those for Ag-Pd/Al_2O_3, no silver sulphate peaks could be seen. These results show that the addition of Pd accelerates the formation of sulphate.

Table 1 shows the BET measurement results and S content for the fresh and poisoned catalysts of Ag-Pd/Al_2O_3 and Ag/Al_2O_3. The data for the pure γ-Al_2O_3 support are also included for comparison. The surface area and the pore volume slightly increase after Ag and Pd are introduced on the support, whereas the pore diameter decreases slightly. However, after the fresh Ag-Pd/Al_2O_3 and Ag/Al_2O_3 catalysts are poisoned by SO_2,

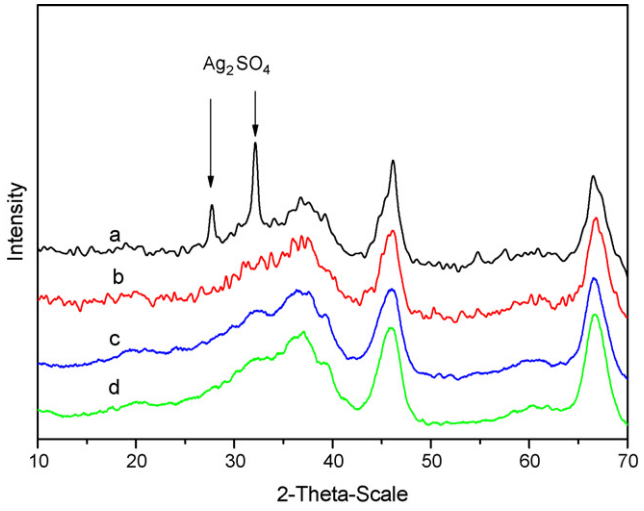

Fig. 2. XRD patterns of the catalyst samples: (a) poisoned Ag-Pd/Al_2O_3, (b) fresh Ag-Pd/Al_2O_3, (c) poisoned Ag/Al_2O_3 and (d) fresh Ag/Al_2O_3.

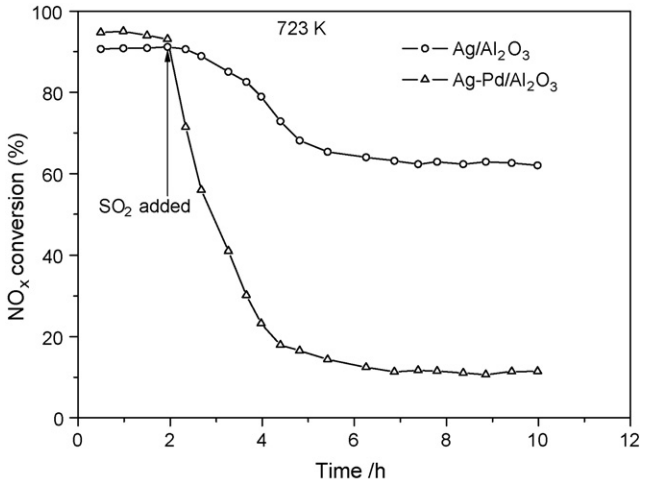

Fig. 3. Time dependence of NO_x conversion during the SCR of NO_x by C_3H_6 over Ag/Al_2O_3 (◯) and $Ag\text{-}Pd/Al_2O_3$ (Δ) at 723 K in the presence of 80 ppm SO_2. Reaction conditions: NO, 800 ppm; C_3H_6, 1714 ppm; O_2, 10 vol%; SO_2, 80 ppm; N_2 balance. $W/F = 0.018$ g s cm^{-3} (GHSV, ~50,000 h^{-1}).

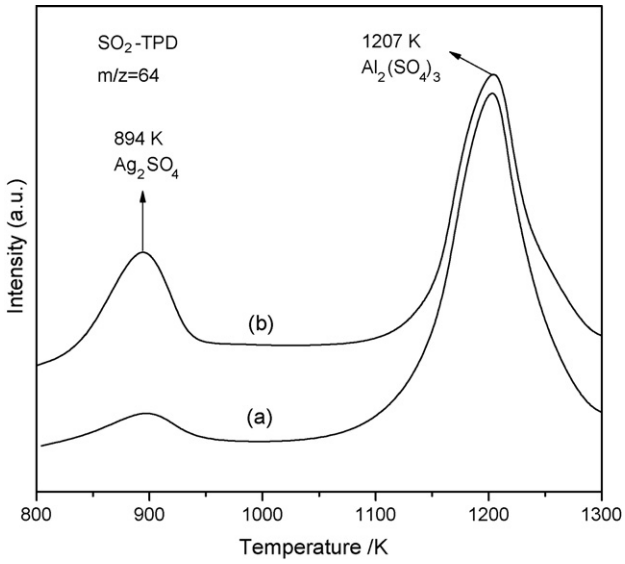

Fig. 4. SO_2-TPD spectra obtained at 64 amu after Ag/Al_2O_3 (a) and $Ag\text{-}Pd/Al_2O_3$ (b) were poisoned by 80 ppm SO_2 for 10 h at 723 K.

significant decreases in the surface area and pore volume are observed. These results demonstrate that the sulphate species are mainly located on the surface of the alumina and that some pores are blocked by the surface sulphate. In addition, the S content of poisoned $Ag\text{-}Pd/Al_2O_3$ is higher than that of the poisoned Ag/Al_2O_3. This result is consistent with the XRD result mentioned above.

3.2. Influence of SO_2 on catalytic activity

The NO_x conversions over the $Ag\text{-}Pd/Al_2O_3$ and Ag/Al_2O_3 catalysts at 723 K were evaluated in a model exhaust gas in the presence/absence of 80 ppm SO_2 as shown in Fig. 3. The initial NO_x conversion in the absence of SO_2 over $Ag\text{-}Pd/Al_2O_3$ and Ag/Al_2O_3 are 96% and 91%, respectively. When SO_2 is introduced to the feed gas stream, the NO_x conversion over both catalysts decreases obviously in the first 2 h. The NO_x conversion is stable at 12% over $Ag\text{-}Pd/Al_2O_3$ catalyst in the presence of SO_2, which is much lower than the stable NO_x conversion of 63% over Ag/Al_2O_3. These results reveal that $Ag\text{-}Pd/Al_2O_3$ is less resistant to sulphur than Ag/Al_2O_3.

3.3. SO_2-TPD

To gain insights into the nature of the species formed on the poisoned samples, we examined TPD experiments for Ag/Al_2O_3 and $Ag\text{-}Pd/Al_2O_3$ after exposure to 80 ppm SO_2 in 10% O_2 at 723 K for 10 h, by monitoring SO_2 ($m/z = 64$) signals. As shown in Fig. 4, SO_2 desorbs in two peaks for poisoned Ag/Al_2O_3, centered at around 894 and 1207 K, respectively. The high-temperature peak centered around 1207 K should be derived from the thermally stable sulphate species formed on Ag/Al_2O_3. According to the previous literature [14,15], $Al_2(SO_4)_3$ was formed through the treatment of alumina with SO_2, and it decomposed to yield alumina oxide at 1162–1223 K. Thus, we can deduce that the higher temperature peak around 1207 K may be attributed to the decomposition of sulphate species formed on Al_2O_3 surface. The peak at 894 K may be attributed to the SO_2 generated by the decomposition of surface sulphate species on the Ag site, which is in accordance with the result of Meunir and Ross [16].

A similar TPD pattern is obtained for poisoned $Ag\text{-}Pd/Al_2O_3$, as shown in the same figure. Compared with the TPD feature of the poisoned Ag/Al_2O_3, the TPD spectrum of the poisoned $Ag\text{-}Pd/Al_2O_3$ shows a strong and broad desorption peak centered at 894 K. This means that the addition of trace Pd promoted the formation of Ag_2SO_4. It is known that Ag site is the reactive site for the SCR of NO_x, and that the formation of Ag_2SO_4 is not favorable for the SCR of NO_x. Therefore, the performance of $Ag\text{-}Pd/Al_2O_3$ is not better than Ag/Al_2O_3 in the presence of SO_2.

3.4. NO-TPD

Fig. 5 shows a comparison of the NO and O_2 TPD profiles for the fresh and SO_2 treated $Ag\text{-}Pd/Al_2O_3$ catalysts. The TPD spectra are markedly changed by the SO_2 treatment. The desorption of NO from the fresh catalyst is observed at 525 and 813 K. The desorption of NO at 813 K is accompanied with desorption of oxygen, which indicates that some nitrate-type surface species decompose into NO and O_2 [17]. The desorption of NO from the SO_2 poisoned sample is observed at temperatures of 465 and 650 K, which are lower than those for the fresh sample, respectively. These results suggest that the nitrates decompose more easily on the poisoned catalyst surface than on the fresh surface.

3.5. FT-IR studies

In order to investigate the mechanism of SO_2 effects on the SCR of NO_x over $Ag\text{-}Pd/Al_2O_3$ catalyst, we also carried out experiments using in situ DRIFTS.

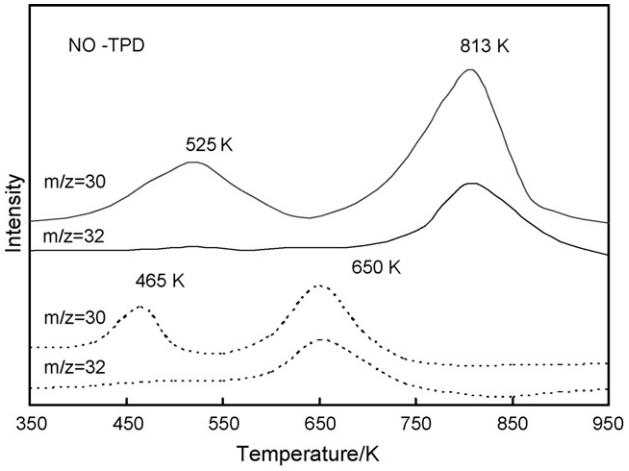

Fig. 5. NO-TPD spectra obtained at 30 amu (NO) and 32 amu (O_2) for fresh sample (solid line) and Ag-Pd/Al_2O_3 poisoned by 80 ppm SO_2 at 723 K for 10 h (broken line). Exposure conditions: samples were exposed to a flow of NO (800 ppm) + O_2 (10%) + N_2 at 473 K for 60 min.

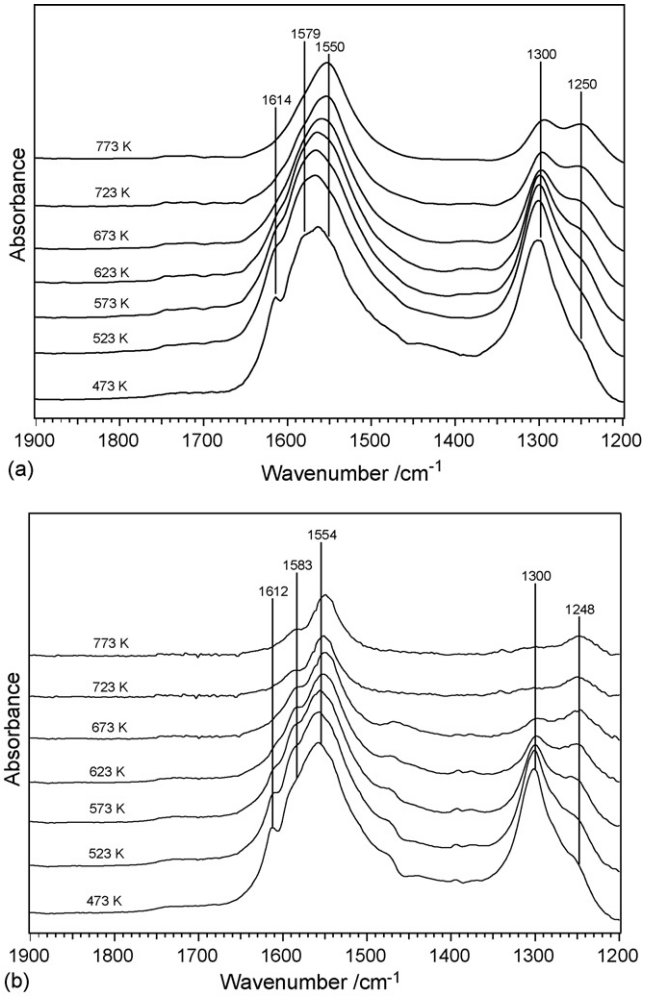

Fig. 6. In situ DRIFTS spectra in a steady state at various temperatures in a flow of NO (800 ppm) + O_2 (10%) + N_2: (a) fresh Ag-Pd/Al_2O_3 and (b) SO_2 poisoned Ag-Pd/Al_2O_3.

Fig. 6(a and b) shows the respective IR spectra of the fresh and poisoned Ag-Pd/Al_2O_3 catalyst in the flow of NO + O_2 in a steady state at various temperatures. Based on previous literatures [4,5,8,18,19], the bands are assigned to monodentate nitrate (1250 or 1248, 1550 cm^{-1}), bidentate nitrate (1300, 1579 or 1583 cm^{-1}) and bridge nitrate (1614 or 1612 cm^{-1}), respectively. The significant difference between Fig. 6(a and b) is the peak intensity at 1300 cm^{-1}. With increasing temperature, the peak at 1300 cm^{-1} for the poisoned sample disappears at 673 K, while it was relatively strong for the fresh sample. On the other hand, the peak intensity at 1550 and 1579 cm^{-1} for the fresh sample is also stronger than that of the poisoned sample. These results suggest that the presence of surface sulphate blocks the NO oxidation on the catalyst surface, which results in the inhibition of NO_3^- formation. These results are in good agreement with the NO-TPD results.

Fig. 7(a and b) shows the respective IR spectra of the fresh and poisoned Ag-Pd/Al_2O_3 catalyst in the flow of NO + C_3H_6 + O_2 in a steady state at various temperatures. The bands in Fig. 7(a and b) are assigned to bands of adsorbed nitrates (1300, 1585 or 1587 cm^{-1}) [4], acetate (1394, 1460–1475, 1572 cm^{-1}) [4,8,18,19], surface enolic species ($H_2C{=}CH{-}O{-}M$) (1637 cm^{-1}) [8,20] and surface –NCO species (2233 or 2235 cm^{-1}) [8]. The surface enolic species is formed by the partial oxidation of C_3H_6 on the Ag-Pd/Al_2O_3 catalyst [8,20]. The enolic surface species is reactive towards nitrate to form the –NCO species [20,21]. The –NCO on Ag-Pd/Al_2O_3 is an important reaction intermediate during the SCR of NO by C_3H_6. By comparison of the relative peak intensities shown in Fig. 7(a and b), we conclude that the surface enolic species and nitrates have a low surface concentration on the SO_2 poisoned Ag-Pd/Al_2O_3 catalyst surface because oxidation processes of both NO and C_3H_6 are blocked by the surface sulphate. Subsequently, this results in the low surface concentration of –NCO species. Therefore, the SO_2 poisoned Ag-Pd/Al_2O_3 catalyst shows a lower activity of NO reduction by C_3H_6 than the fresh sample. On the other hand, a large negative peak at 1394 cm^{-1} is observed in Fig. 7(b), which is related to the site of sulphate adsorption [22]. This is because we used the SO_2 poisoned sample as the background in the experiment of Fig. 7(b).

Fig. 8 shows the SO_2 effect on the DRIFTS spectra of Ag-Pd/Al_2O_3 during the SCR of NO_x at 723 K. The bottom spectrum was taken after 1 h under SO_2-free flow and the next four spectra were taken every half hour in the presence of 80 ppm SO_2. The bands of surface –NCO (2233 cm^{-1}), enolic species (1637 cm^{-1}), acetate (1462 cm^{-1}) and nitrate (1300 cm^{-1}) can be observed. After SO_2 exposure, there is a peak at ~1344 cm^{-1} growing in intensity with time. According to literatures [19,23–25], the band at ~1344 cm^{-1} can be attributed to asymmetric stretching vibrations of OSO of sulphate related to Al phase. With increasing SO_2 exposure, the bands at ~1344 cm^{-1} shift to high wavenumber of 1358 cm^{-1}, because of the accumulation of sulphate on the catalyst surface [25]. This is the reason why a negative peak at 1394 cm^{-1} appears when the poisoned catalyst is used. At the same time, the sulphate peak at 1344–1358 cm^{-1} is very strong, which may be a reason why the peak related to Ag phase (1313 cm^{-1}) cannot be

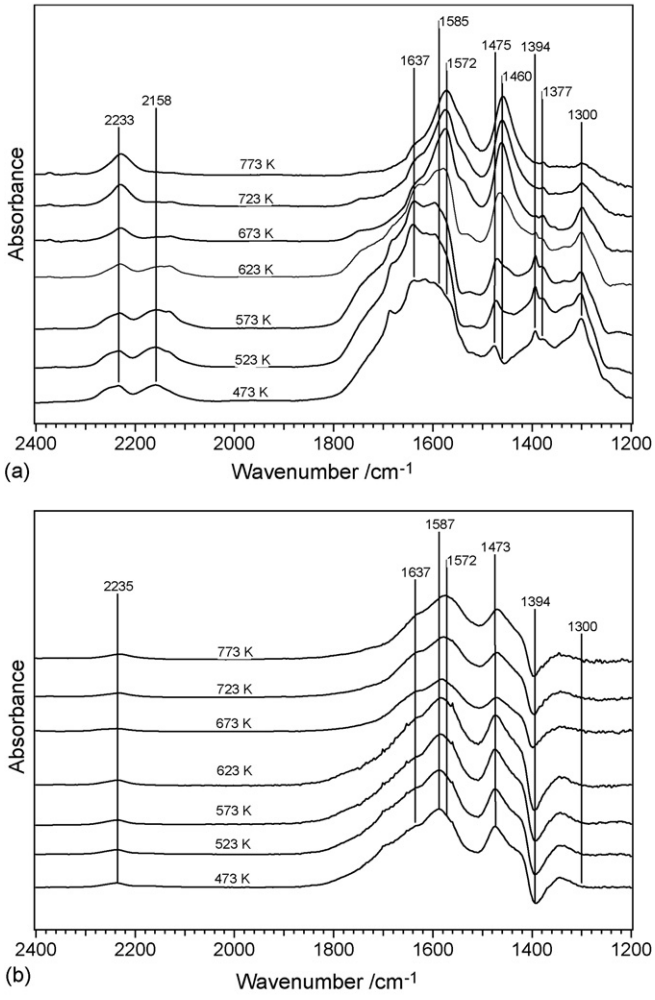

Fig. 7. In situ DRIFTS spectra during the SCR of NO_x at various temperatures. Reaction conditions: NO, 800 ppm; C_3H_6, 1714 ppm; O_2, 10%; N_2 balance: (a) fresh Ag-Pd/Al_2O_3 and (b) SO_2 poisoned Ag-Pd/Al_2O_3.

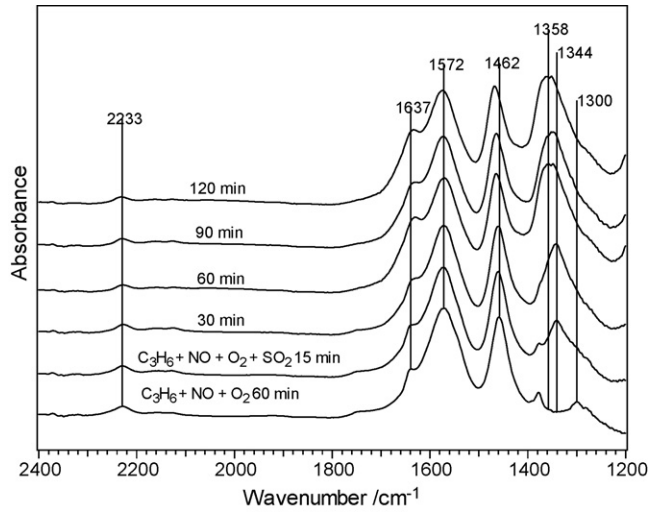

Fig. 8. Dynamic changes of in situ DRIFTS spectra of Ag-Pd/Al_2O_3 as a function of time during the SCR of NO_x at 723 K by addition of 80 ppm SO_2. Reaction conditions: NO, 800 ppm; C_3H_6, 1714 ppm; O_2, 10%; N_2 balance.

clearly seen. The peaks at 2233 and 1300 cm^{-1} decrease dramatically, and almost disappears after 2 h of SO_2 exposure. These results indicate that the sulphate on the Ag-Pd/Al_2O_3 catalyst surface blocks the formation of NO_3^- and then the formation of –NCO. In addition, and that the band of enolic species at 1637 cm^{-1} slightly increases. This is partially due to the following step of enolic species reaction to nitrates being blocked, which implies that the enolic species accumulates on the catalyst surface. The other reason may be the introduction of $SO_2(+O_2)$ creating Brφnsted acid sites [26], which can activate the propene. It can be concluded when the enolic species is previously formed on the catalyst surface, the introduction of SO_2 could not influence the formation of the enolic species. However, when the surface is previously covered by sulphate, the formation of enolic species will be suppressed. That is why the concentration of the enolic species is much lower over SO_2 poisoned Ag-Pd/Al_2O_3 than that over the fresh catalyst (Fig. 7 (b)). Under the same condition as Fig. 8, a similar phenomenon is observed over the Ag/Al_2O_3 catalyst [27]. However, large amount of sulphate appears on Ag-Pd/Al_2O_3 compared to Ag/Al_2O_3, which is consistent with the results of ICP-OES, XRD and SO_2-TPD.

4. Conclusion

Ag-Pd/Al_2O_3 showed a good performance in SCR of NO_x in the absence of SO_2. However, the presence of SO_2 in the feed gas led to a permanent deactivation of the SCR of NO_x by C_3H_6 over the Ag-Pd/Al_2O_3 catalyst at 723 K. The formation of surface sulphates was observed on both the alumina and silver phases. The presence of Ag_2SO_4 and $Al_2(SO_4)_3$ species inhibited the formation of enolic and NO_3^- species, and subsequently inhibited the formation of surface –NCO. Compared with Ag/Al_2O_3, the addition of trace Pd promoted Ag_2SO_4 formation on the reactive Ag site, which may be the main reason why Ag-Pd/Al_2O_3 showed lower SO_2 tolerance than Ag/Al_2O_3. It is suggested that the addition of noble metals may not be an appropriate method for improving the SO_2 resistance of Ag/Al_2O_3.

Acknowledgements

This work was financially supported by the National Science Fund for Distinguished Young Scholars of China (20425722) and Key Program of NNSFC (20437010).

References

[1] T. Miyadera, Appl. Catal. B 2 (1993) 199–205.
[2] K. Shimizu, H. Maeshima, A. Satsuma, T. Hattori, Appl. Catal. B 18 (1998) 163–170.
[3] S. Sumiya, H. He, A. Abe, N. Takezawa, K. Yoshida, J. Chem. Soc. Faraday Trans. 94 (1998) 2217–2219.
[4] F.C. Meunier, J.P. Breen, V. Zuzaniuk, M. Olsson, J.R.H. Ross, J. Catal. 187 (1999) 493–505.
[5] F.C. Meunier, V. Zuzaniuk, J.P. Breen, M. Olsson, J.R.H. Ross, Catal. Today 59 (2000) 287–304.
[6] S. Kameoka, Y. Ukisu, T. Miyadera, Phys. Chem. Chem. Phys. 2 (2000) 367–372.
[7] H. He, Y. Yu, Catal. Today 100 (2005) 37–47.
[8] H. He, J. Wang, Q. Feng, Appl. Catal. B 46 (2003) 365–370.

[9] J. Wang, H. He, S. Xie, Y. Yu, Catal. Commun. 6 (2005) 195–200.
[10] G. Corro, J.L.G. Fierro, R. Montiel, S. Castillo, M. Moran, Appl. Catal. B 46 (2003) 307–317.
[11] S. Sumiya, M. Saito, H. He, Q. Feng, N. Takezawa, Catal. Lett. 50 (1998) 87–91.
[12] T.N. Angelidis, N. Kruse, Appl. Catal. B 34 (2001) 201–212.
[13] H.S. Gandhi, M. Shelef, Appl. Catal. 77 (1991) 175–186.
[14] T. Yang, T. Chang, C. Yeh, J. Mol. Catal. A 123 (1997) 163–169.
[15] F. Chang, M. Tsay, M. Kuo, C. Yang, Appl. Catal. A 226 (2002) 213–224.
[16] F.C. Meunir, J.R.H. Ross, Appl. Catal. B 24 (2000) 23–32.
[17] J. Li, J. Hao, L. Fu, Z. Liu, X. Cui, Catal. Today 90 (2004) 215–221.
[18] K. Shimizu, J. Shibata, A. Satsuma, T. Hattori, Phys. Chem. Chem. Phys. 3 (2001) 880–884.
[19] K. Shimizu, T. Higashimata, M. Tsuzuki, A. Satsuma, J. Catal. 239 (2006) 117–124.
[20] Y. Yu, H. He, Q. Feng, J. Phys. Chem. B 107 (2003) 13090–13092.
[21] Q. Wu, H. He, Y. Yu, Appl. Catal. B 61 (2005) 107–113.
[22] R.T. Yang, N. Tharappiwattananon, R.Q. Long, Appl. Catal. B 19 (1998) 289–304.
[23] P. Decyk, D.K. Kim, S.I. Woo, J. Catal. 203 (2001) 369–374.
[24] J.M. Watson, U.S. Ozkan, J. Catal. 217 (2003) 1–11.
[25] Q. Wu, H. Gao, H. He, J. Phys. Chem. B 110 (2006) 8320–8324.
[26] M. Ziolek, J. Kujawa, O. Saur, A. Aboulayt, J.C. Lavalley, J. Mol. Catal. A 112 (1996) 125–132.
[27] Q. Wu, H. Gao, H. He, Chin. J. Catal. 27 (2006) 403–408.